



# Genotype-phenotype Correlations of Ocular Posterior Segment Abnormalities in Marfan Syndrome

Yan Liu, BM,<sup>1,2,3,4,\*</sup> Yuqiao Ju, MM,<sup>1,2,3,4,\*</sup> Tian-hui Chen, MM,<sup>1,2,3,4</sup> Yong-xiang Jiang, MD, PhD<sup>1,2,3,4</sup>

**Purpose:** Marfan syndrome (MFS) is a connective tissue disorder caused by mutations in the *fibrillin-1* (*FBN1*). In addition to typical phenotypes such as ectopia lentis (EL) and aortic dilation, patients with MFS are prone to ocular posterior segment abnormalities, including retinal detachment (RD), maculopathy, and posterior staphyloma (PS). This study aims to investigate the correlations between *FBN1* genotype and posterior segment abnormalities within a Chinese cohort of MFS.

**Design:** Retrospective study.

**Participants:** One hundred twenty-one eyes of 121 patients with confirmed *FBN1* mutations between January 2015 and May 2023 were included.

**Methods:** Comprehensive ophthalmic examination findings were reviewed, and the incidence of RD, atrophic, tractional, and neovascular maculopathy (ATN classification system), and PS was analyzed between different genotype groups. Only the more severely affected eye from each patient was included.

**Main Outcome Measures:** Clinical features and risk factors.

**Results:** Of 121 patients, 60 eyes (49.59%) exhibited posterior segment abnormalities, including RD (4, 3.31%), maculopathy (47, 38.84%), and PS (54, 44.63%). The mean age was  $11.53 \pm 11.66$  years, with 79.34% of patients <20 years old. The location and region of mutations were found to be associated with the incidence of maculopathy ( $P = 0.013$ ,  $P = 0.033$ ) and PS ( $P = 0.043$ ,  $P = 0.036$ ). Mutations in the middle region had a lower incidence of maculopathy and PS ( $P = 0.028$  and  $P = 0.006$ , respectively) than those in C-terminal region. Mutations in the transforming growth factor- $\beta$  (TGF- $\beta$ ) regulating sequence exhibited a higher incidence of maculopathy and PS ( $P = 0.020$ ,  $P = 0.040$ ). Importantly, the location and region of mutations were also associated with the incidence of atrophic maculopathy ( $P = 0.013$  and  $P = 0.033$ , respectively). Mutations in the middle region had a significantly lower probability of atrophic maculopathy ( $P = 0.006$ ), while mutations in the TGF- $\beta$  regulating region had a higher incidence of atrophic maculopathy ( $P = 0.020$ ).

**Conclusions:** Maculopathy and PS were associated with the location and region of *FBN1* mutations. Patients with mutations in the TGF- $\beta$  regulating region faced an increased risk of developing retinopathy.

**Financial Disclosure(s):** Proprietary or commercial disclosure may be found in the Footnotes and Disclosures at the end of this article. *Ophthalmology Science* 2024;4:100526 © 2024 by the American Academy of Ophthalmology. This is an open access article under the CC BY-NC-ND license (<http://creativecommons.org/licenses/by-nc-nd/4.0/>).

Marfan syndrome (MFS) is a relatively rare autosomal dominant genetic disorder, impacting approximately 1 in 5000 individuals.<sup>1,2</sup> Predominantly, around 97% of MFS cases arise from mutations in the pathogenic gene *fibrillin-1* (*FBN1*) (Online Mendelian Inheritance in Man #134797), revealing a spectrum of over 3000 reported mutations, each linked to a distinct array of phenotypes.<sup>3</sup> Consequently, the phenotypes of MFS are diverse, ranging from the common occurrences like ectopia lentis (EL), aortic dilation, and skeletal abnormalities to rarer instances of posterior staphyloma (PS), retinal detachment (RD), and maculopathy. Understanding the correlation between genotypes and phenotypes is pivotal.<sup>4–6</sup>

Maculopathy refers to macular alteration that are characterized by atrophy, traction, and neovascularization, potentially leading to irreversible macular photoreceptor

damage and central visual loss. A primary cause of maculopathy is PS. Posterior staphyloma has a radius of curvature smaller than the peripheral curvature of the eyeball, like a local outpouching of the eyeball. Posterior staphyloma is common in, but not limited to, patients of high myopia.<sup>7,8</sup> In addition to maculopathy, individuals with MFS are more predisposed to the development of RD compared with the general population.<sup>9</sup> Retinal detachment is one of the most severe and prevalent sight-threatening complications, impacting 5% to 11% of all patients with MFS.<sup>4–6,9,10</sup>

Previous studies have extensively demonstrated correlations between *FBN1* genotypes and phenotypes. Mutation in in-frame regions are more likely to develop EL.<sup>11</sup> Longer axial length (AL) was associated with mutations in cysteine residues, calcium-binding epidermal growth factor (cbEGF)-like domain, C-terminal region, and transforming

growth factor  $\beta$  (TGF- $\beta$ ) regulating region.<sup>12,13</sup> Furthermore, mutations in functional regions tend to exhibit severe ocular and systematic manifestations, with neonatal mutations carrying a significantly poorer prognosis than in other regions.<sup>14–17</sup> These findings suggest significant correlations between specific *FBNI* mutations and phenotype.<sup>18–20</sup> However, it remains unclear whether such correlations extend to ocular posterior segment phenotypes in MFS; there is a lack of research specifically addressing the correlation between *FBNI* mutations and posterior segment manifestations.<sup>21</sup> Discovering the correlations is crucial for developing personalized surgical and clinical management strategies, enabling early identification of individuals to improve the prognosis.<sup>22</sup>

This study intended to investigate the influence of genotypes on the onset and development of ocular posterior segment abnormalities in MFS patients, and determine the higher risk genotypes to raise clinical awareness of the seriousness of posterior segment lesions.

## Method

### Patient Eligibility and Ethics Statement

This retrospective clinical observational study adhered to the principles outlined in the Declaration of Helsinki and received approval from the Human Research Ethics Committee of the Eye and ENT Hospital of Fudan University (ChiCTR2000039132). Written informed consent was obtained from all participants or their guardians in subjects <18 years old.

Patients with MFS visiting the Eye and ENT Hospital of Fudan University from January 2015 to May 2023 were initially recruited. The diagnosis of MFS was according to Ghent-2 nosology.<sup>23</sup> Patients with a heterozygous pathogenic *FBNI* mutation and sufficient clinical information were selected. Patients with complex mutations or a history of trauma in either eye were excluded from the study.<sup>24,25</sup> To avoid potential selection bias resulting from familial clustering, only the probands from pedigrees were analyzed. To address high binocular correlation, only the more severely affected eye from each proband was included.

### Ophthalmic Examinations

Full ophthalmic examinations were conducted. Axial length, corneal astigmatism, and corneal mean keratometry were measured using partial coherence interferometry (IOL-Master 700, Carl Zeiss Meditec AG) and rotating Scheimpflug camera (Pentacam, Oculus Optikgeräte GmbH). Intraocular pressure was measured with noncontact tonometer (CT-80, Topcon Medical Systems). Posterior staphyloma was detected by B-scan ultrasonography, fundus photography (CLARUS 500, Carl Zeiss Meditec AG), and OCT (Spectralis OCT, Heidelberg Engineering and Cirrus OCT, Carl Zeiss Meditec). When the ocular accommodation is in a relaxed state, individuals exhibiting a spherical equivalent refractive error of  $\leq -6.00$  diopters are categorized as having high myopia.<sup>26</sup> The classification of

atrophic, tractional, and neovascular maculopathy (ATN classification system) was based on OCT, fundus photography, and ultrawidefield fundus imaging (Daytona, Optos, Inc. Enterprise Way).<sup>27,28</sup> All patients were examined by board-certified optometrists and ophthalmologists. Medical and family histories were meticulously documented.

### Genetic Screening

All genomic DNA samples were extracted from peripheral blood of all probands. Panel-based next-generation sequencing was performed, as previously reported, covering the exon sequences of 289 genes associated with common inherited eye diseases.<sup>25</sup> Multiplex ligation-dependent probe amplification was performed using SALSA MLPA Probeset Kits (P065-C1/P066-C1, MRC-Holland) for patients with suspected *FBNI* mutations.<sup>25</sup> Variants with minor allele frequencies of  $<0.05$  were selected for further analysis. The candidate causal gene variants thereby discovered were confirmed by Sanger sequencing, and primers were designed using the Primer V.3.0 website (<http://primer3.ut.ee/>). Mutations were annotated based on biological information analysis, and mutant sites were selected based on clinical manifestations. Protein and genomic structures were mapped for all variants using IBS1.0.3 illustrator.

### Genotype-Phenotype Analysis

All 121 patients were enrolled in the genotype-phenotype analysis. Maculopathy, PS, and RD were all within our scope of study. Mutations were classified following the American College of Medical Genetics and Genomics guidelines. Premature termination codons include nonsense, out-of-frame insertions or deletions, and complete allele deletions, in-frame mutations include missense mutations, in-frame insertions or deletions, in-frame splicing variants, and in-frame intragenic duplications. The location criteria were based on protein location, including the N-terminal region (exon 1–21), middle region (exons 22–42), and C-terminal region (exon 43–65). Patients were classified into 3 groups: cysteine-creating, cysteine-eliminating, and other amino acids alterations. Missense mutations were mapped to specific regions, including the neonatal region, TGF- $\beta$  regulating region, TGF- $\beta$  binding region, latent TGF- $\beta$  binding protein (LTBP) region, and C-N interaction site region. The particular region, TGF- $\beta$  regulating sequence, was compared with mutations located elsewhere.<sup>15,29</sup> Missense mutations were classified based on the function domains, including cbEGF-like, epidermal growth factor-like, Hybrid module, TGF- $\beta$  binding protein (TGFBP), and 4-cys motif LTBP like domains. Protein domains were mapped using the Universal Mutation Database-*FBNI* database (<http://umd.be/FBNI/>), as described in our published articles.<sup>14,15</sup>

### Statistical Analysis

IBM Statistics SPSS version 22.0 (IBM Corp) was used for all statistical analysis. Continuous variables were presented

as means  $\pm$  standard deviation, while categorical variables were described as counts or proportions. Chi-square test, Yates' correction, or Fisher exact test was employed to compare the category variables. The Wilcoxon Mann-Whitney *U* tests and Kruskal-Wallis test were employed to compare the incidence of different maculopathy types among different mutation groups. Binomial logistic regression analysis was performed to analyze the correlation of different mutation groups and ocular abnormalities present, while ordinal logistic regression analyses were constructed with atrophic maculopathy, tractional maculopathy, and neovascular maculopathy as the dependent variable to assess the association with genotypes. Unmeasurable or unreliable values because of incoordination or incorporation were annotated as missing.  $P < 0.05$  was the threshold of statistical significance.

## Results

### Cohort Demographics

Table 1 summarizes the demographic and clinical characteristics of the 121 enrolled eyes. The mean age of the cohort was  $11.53 \pm 11.66$  years, comprised 76 males and 45 females, and 79.34% of the patients were  $<20$  years old. Thirty-six point thirty-six percent of patients had a positive family history of MFS. The enrolled eyes exhibited deviations from normal reference ranges in Z-score of AL ( $1.73 \pm 3.43$  mm), intraocular pressure ( $14.59 \pm 3.19$  mmHg), corneal mean keratometry ( $39.69 \pm 2.48$  diopters), and corneal astigmatism ( $1.88 \pm 0.98$  diopters).<sup>18,19,30</sup> The AL was  $23.49 \pm 6.27$  mm, and the average white to white was  $12.04 \pm 0.58$  mm. Among the study sample, 60 eyes (49.59%) had retinopathy and 98 eyes (80.99%) had EL. Posterior staphyloma was detected in 54 eyes (44.63%) and maculopathy in 47 eyes (38.34%). Other comorbidities included microspherophakia (10, 8.26%), macrophthalmia (2, 1.65%), cataract (7, 5.79%), ciliary body cyst (6, 4.96%), and glaucoma (1, 0.83%). Moreover, high myopia was identified in 61.98% of the examined eyes. Figure 1A–I provides fundus photography and OCT examples of enrolled eyes with different maculopathy types and RD. Figure 1J showed the proportion of ATN classification, with 3.31% of eyes ultimately developing RD in the last follow-up data.

### Genetic Analysis

A total of 100 different mutations in 121 patients (including 11 recurrent mutations in 32 patients) were detected (Fig 2). The most prevalent mutation was c.184C>T/p. Arg 62 Cys in exon 2 and 4-cys motif LTBP like domain (7/121, 5.79%). Figure 2A illustrates the site of *FBN1* mutations in this cohort and the structure of fibrillin-1. Figure 2B shows the frequency of *FBN1* mutations per exon. Figure 2C marks 4 mutations not included in previous studies. Cross-analysis of each genotype revealed that 45 patients with cysteine-eliminating mutations had mutations in the cbEGF-like

Table 1. Demographical Characteristic and Baseline Characteristic of 121 Enrolled Eyes

Characteristics	Mean $\pm$ Standard Deviation (Range) or Number (%)	
Demographics		
Sex (male/female)	76/45	
Age group	$11.53 \pm 11.66$	
	$<20$	96 (79.34%)
	$\geq 20$	25 (20.66%)
Family history	Positive	44 (36.36%)
	Negative	77 (63.64%)
Ocular biometrics	Right/left	64/57
	Ectopia lentis	98 (80.99%)
	High myopia	75 (61.98%)
	AL/mm	$23.49 \pm 6.27$
	Z-AL	$1.73 \pm 3.43$
	BCVA, logMAR	$0.89 \pm 0.33$
	IOP/mmHg	$14.59 \pm 3.19$
	ACD/mm	$3.12 \pm 0.59$
	WTW/mm	$12.04 \pm 0.58$
	Km/D	$39.69 \pm 2.48$
	AST/D	$1.88 \pm 0.98$
Comorbidity	Posterior staphyloma	54 (44.63%)
	Maculopathy	47 (38.84%)
	Retinal detachment	4 (3.31%)

ACD = anterior chamber depth; AL = axial length; AST = corneal astigmatism; BCVA = best corrected visual acuity; IOP = intraocular pressure; Km = mean keratometry; logMAR = logarithm of minimal angle of resolution; WTW = white-to-white measurement; Z-AL = Z-score of axial length.

domain, and 30 patients with cysteine-eliminating mutations had mutations in the N-terminal region. Additionally, 14 patients had mutations located in the LTBP region and belonged to cysteine-creating mutations (Fig 2D–G). The majority were primarily distributed in the N-terminal region (60, 49.59%) and middle region (43, 35.54%) (Fig 3C). Among these patients, the most common mutations were missense (112, 92.56%), followed by nonsense (4, 3.25%) (Fig 3B). Additionally, 60.71% of missense mutations affected cbEGF-like domains (Fig 3E). Among the 112 patients with missense mutations, 83.04% involved cysteine, with 56.25% being cysteine-eliminating mutations and 26.79% being cysteine-creating mutations (Fig 3D). Furthermore, 111 (99.11%) patients had mutations in exact protein domains, and 78 (58.75%) patients had mutations in functional regions (Fig 3E, F).

### Incidence of Maculopathy and PS With *FBN1* Mutations

The incidence of specific ocular comorbidities was analyzed for different mutation groups. The positive rate of maculopathy was significantly associated with the mutation location and region ( $P = 0.013$  and  $P = 0.033$ , respectively), as well as the incidence of PS ( $P = 0.043$  and  $P = 0.036$ , respectively) (Table 2). In comparison with mutations in the C-terminal region, patients with mutations in the middle region had a lower risk of

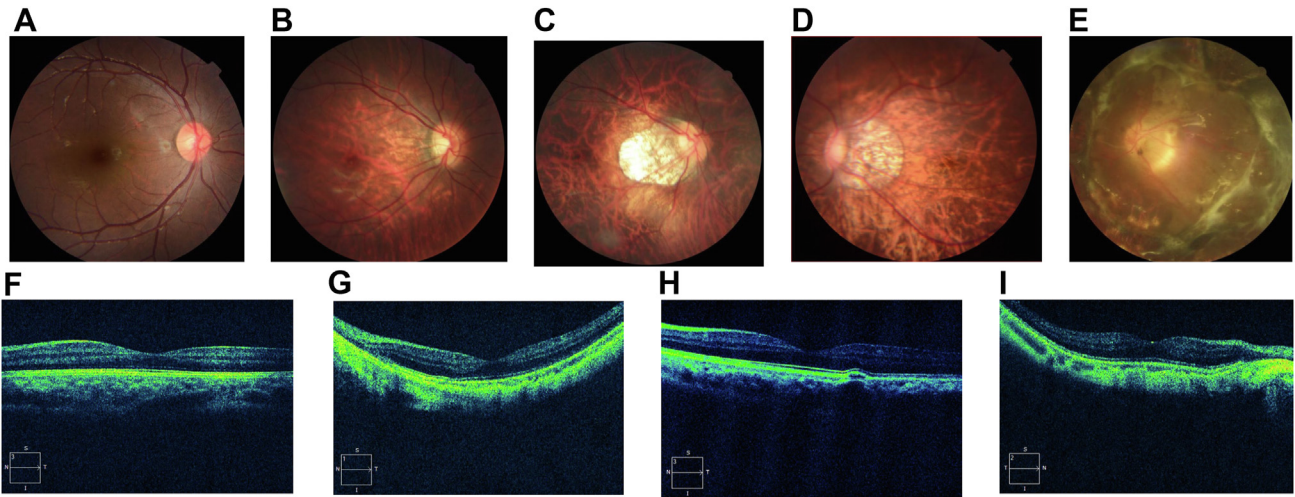


**Figure 1.** Clinical presentation of patients with *FBN1* mutations and the proportion of atrophic, tractional, and neovascular maculopathy classification and retinal detachment. **A**, Right eye in a 7-year-old patient with Marfan syndrome (MFS) without myopic retinal lesions (A0). **B**, Right eye in a 12-year-old patient with MFS with tessellated fundus only (A1). **C**, Right eye in a 17-year-old patient with MFS with diffuse chorioretinal atrophy (A2). **D**, Left eye in an 11-year-old patient with MFS with patchy chorioretinal atrophy (A3). **E**, OCT of an 8-year-old patient with MFS without macular schisis (T0). **F**, OCT of an 11-year-old patient with MFS with outer foveoschisis (T1). **G**, OCT of a 32-year-old patient with MFS with active choroidal neovascularization (N2a). **H**, OCT of a 17-year-old patient with MFS with Scar/Fuch's spot (N2s). **I**, Left eye in a 17-year-old patient with MFS with retinal detachment and diffuse chorioretinal atrophy.

developing maculopathy ( $P = 0.028$ , odds ratio [OR] 0.276, 95% confidence interval [CI] 0.087–0.871) and PS ( $P = 0.006$ , OR 0.193, 95% CI 0.059–0.629). Mutations in the TGF- $\beta$  regulating sequence region, in particular, seemed

to have a higher risk of maculopathy ( $P = 0.020$ , OR 12.536, 95% CI 1.501–104.67) and PS ( $P = 0.040$ , OR 9.273, 95% CI 1.112–77.31) (Table 3). No significant differences were found in other groups.

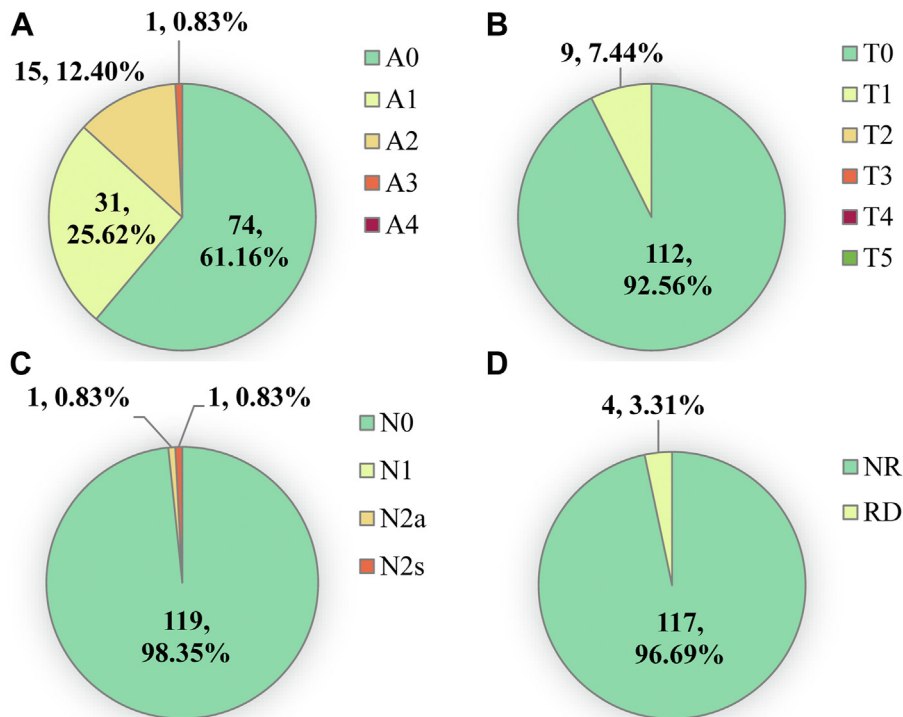


**Figure 2.** Proportion of atrophic, tractional, and neovascular maculopathy classification and retinal detachment. **A**, Distribution of atrophic (A) maculopathy. **B**, Distribution of tractional (T) maculopathy. **C**, Distribution of neovascular (N) maculopathy. **D**, Distribution of retinal detachment. NR = no retinal detachment; RD = retinal detachment.



Table 2. Relationship Between Posterior Segment Comorbidities and *FBN1* Genotype

Genotype	Maculopathy		Posterior Staphyloma	
	Positive (%)	P	Positive (%)	P
Location				
C-terminal region	11 (61.1%)	<b>0.013*</b>	11 (61.1%)	<b>0.043*</b>
Middle region	10 (23.3%)		13 (30.2%)	
N-terminal region	26 (43.3%)		30 (50.0%)	
Type				
In-frame	45 (39.1%)	1.000 <sup>†</sup>	51 (44.3%)	1.000 <sup>†</sup>
PTC	2 (33.3%)		3 (50.0%)	
Cysteine				
Other amino acid	5 (26.3%)	0.114*	9 (47.4%)	0.131 <sup>†</sup>
Creating	9 (30.0%)		9 (30.0%)	
Eliminating	30 (47.6%)		32 (50.8%)	
Domain				
cbEGF-like	28 (41.2%)	0.257 <sup>†</sup>	30 (44.1%)	0.163 <sup>†</sup>
EGF-like	7 (58.3%)		8 (66.7%)	
Hybrid module	3 (25.0%)		5 (41.7%)	
TGFβP	2 (18.2%)		2 (18.2%)	
4-cys motif LTBP-like	4 (50.0%)		5 (62.5%)	
Region				
TGF-β regulating	9 (90.0%)	<b>0.033<sup>†</sup></b>	9 (90.0%)	<b>0.036<sup>†</sup></b>
Neonatal region	7 (36.8%)		8 (42.1%)	
TGF-β binding	8 (40.0%)		8 (40.0%)	
LTBP	13 (46.4%)		17 (60.7%)	
C-N interaction site	0 (0.0%)		0 (0.0%)	

cbEGF = calcium-binding epidermal growth factor; *FBN1* = fibrillin-1; LTBP = latent transforming growth factor β binding protein; PTC = premature termination codon; TGFβP = transforming growth factor β binding protein; TGF-β = transforming growth factor β.

Bold type indicates *P* values less than 0.05.

\*Pearson chi-squared tests.

<sup>†</sup>Fisher exact test.

atrophic maculopathy than in other regions ( $P = 0.022$ , OR 1.476 95% CI 0.214–2.738) (Fig. 5). No statistical differences were found in other groups.

## Discussion

Marfan syndrome presents a complex array of genetic mutations and diverse phenotypic manifestations, posing a considerable challenge to clinicians and researchers in the quest to identify diagnostic patterns that can enhance patient diagnosis, treatment outcomes, and long-term prognosis. Ocular involvement stands out as a prominent diagnostic feature, including EL, myopia, glaucoma, peripheral retinal degeneration, rhegmatogenous detachment, and early cataracts.<sup>6,31,32</sup> In this study, we intended to characterize posterior segment manifestations in patients with MFS and explore their associations with *FBN1* mutations, as the understanding of posterior segment phenotype in MFS was lacking.

Consistent with prior research, missense mutations predominated, with cysteine alterations being particularly frequent.<sup>33,34</sup> Generally, variants causing in-frame loss or gain of central coding sequence through deletions, insertions, or splicing errors were associated with severe,

early-onset, and rapidly progressive MFS, contributing to an increased prevalence of retinopathy.<sup>33,34</sup> Nevertheless, in our study, correlations were identified only in the location and region of mutations.

Mutations in the C-terminal region showed a higher risk of posterior segment lesions.<sup>35,36</sup> The C-terminal propeptide is an essential requirement for the secretion of full length fibrillin-1 from cells.<sup>36</sup> Fibrillin-1, a structural macromolecule that acts as a scaffold for elastin deposition, can form microfibrils and elastic fibers that enhance the flexibility and strength of connective tissue.<sup>37</sup> The phenotypic variability depends on the threshold of functional microfibrils in the zonules and other tissues. Affected individuals typically exhibit residual levels well below 50% of the normal level. Besides quantitative defects, *FBN1* mutations can also disrupt the structure or homeostasis of growth factors, and even the export of fibrillin to the extracellular matrix.

A higher frequency of missense mutations involves cysteine residues and 5' end mutations. Cysteine residues are distributed extensively throughout fibrillin-1, with a presence noted at >360 locations within the protein's structure. Notably, these positions are predominantly clustered within the first 15 exons responsible for encoding the N-terminal region of fibrillin-1. The formation of disulfide bridges at these cysteine residues assumes a critical role in shaping the protein's tertiary structure, ultimately influencing the formation of homodimer. Elimination of cysteine residues in individuals results in normal levels of fibrillin synthesis; however, there is a significant reduction in matrix deposition, indicative of disulfide bonding disruption. This disruption, in turn, impacts the structural integrity of the lens zonules.<sup>38</sup>

One hallmark feature of MFS is an increased activated TGF-β expression. Our study indicated that mutations in the TGF-β regulating sequence showed a promotive effect on the occurrence of PS and maculopathy.<sup>39</sup> Mutations affecting the TGF-β domain act through LTBPs, resulting in altered TGF-β signaling.<sup>2</sup> The TGF-β regulating sequence strongly and specially interacts with the N-terminal of *FBN1* and the C-terminal of LTBP. This interaction sequesters TGF-β in its inactive form. Furthermore, fibrillin-1 also regulate the bioavailability of TGF-β1, thereby preventing TGF-β1 and Smad2 signaling from optimal activation, resulting in elevated levels of active TGF-β and increased TGF-β expression and activation.<sup>29,40</sup> This upregulation exacerbates fibrosis by significantly reducing microfibrils deposited by peripheral tissues and fibroblasts in the matrix, accompanied by increasing free collagen fibers and enhancing protease activity within the extracellular matrix. Studies have also shown that the TGF-β signaling might involve the pathogenesis of elastin-associated *FBN1* in the scleral and retina.<sup>41,42</sup>

Retinopathy refers to pathological alterations to the retina, arising from a range of causes, including environmental factors and genetic predispositions.<sup>43</sup> Various forms of retinopathy represent leading global causes of vision loss. Previous studies have shown that fibrillin-1/microfibril associated glycoprotein 1 performs essential functions in retinal arteriolar integrity and defects induced by *FBN1* mutations can be prevented or partially rescued pharmacologically. Additionally, tortuous retinal vessels were

Table 3. Logistic Regression Analysis Between Posterior Segment Comorbidities and *FBN1* Genotype

	Maculopathy				Posterior Staphyloma			
	P	OR	95% CI		P	OR	95% CI	
Location								
C-terminal region*	<b>0.048</b>				<b>0.017</b>			
Middle region	<b>0.028</b>	0.276	0.087	0.871	<b>0.006</b>	0.193	0.059	0.629
N-terminal region	0.410	0.636	0.217	1.863	0.190	0.487	0.166	1.428
Type								
In-frame*								
PTC	0.786	1.255	0.243	6.482	0.777	0.778	0.137	4.423
Cysteine								
Other*	0.171				0.124			
Creating	0.222	0.476	0.145	1.568	0.781	1.200	0.332	4.340
Eliminating	0.794	1.147	0.411	3.203	0.107	2.545	0.819	7.916
Domain								
cbEGF-like*	0.285				0.205			
EGF-like	0.634	0.700	0.161	3.037	0.332	0.474	0.105	2.143
Hybrid module	0.714	1.400	0.232	8.464	0.848	1.200	0.185	7.770
TGFBP	0.258	0.333	0.050	2.239	0.365	0.429	0.068	2.684
4-cys motif LTBP like	0.154	0.222	0.028	1.754	0.060	0.133	0.016	1.085
Region								
Other regions*								
TGF- $\beta$ regulating	<b>0.020</b>	12.536	1.501	104.67	<b>0.040</b>	9.273	1.112	77.31

CI = confidence interval; cbEGF = calcium-binding epidermal growth factor; *FBN1* = fibrillin-1; LTBP = latent transforming growth factor  $\beta$  binding protein; OR = odds ratio; PTC = premature termination codon; TGFBP = transforming growth factor  $\beta$  binding protein; TGF- $\beta$  = transforming growth factor  $\beta$ .

Bold type indicates *P* values less than 0.05.

\*Control group.

Table 4. Relationship Between the Incidence of MFS Maculopathy (ATN) and *FBN1* Genotype

Genotype	Atrophic Maculopathy		Tractional Maculopathy		Neovascular Maculopathy	
	Positive (%)	P	Positive (%)	P	Positive (%)	P
Location						
C-terminal region	11 (61.1%)	<b>0.013*</b>	2 (11.1%)	0.628 <sup>†</sup>	1 (5.6%)	0.401 <sup>‡</sup>
Middle region	10 (23.3%)		2 (4.7%)		0 (0.0%)	
N-terminal region	26 (43.3%)		5 (8.3%)		1 (1.7%)	
Type						
In-frame	45 (39.1%)	0.774 <sup>†</sup>	9 (7.8%)	0.329 <sup>†</sup>	2 (1.7%)	1.000 <sup>‡</sup>
PTC	2 (33.3%)		0 (0.0%)		0 (0.0%)	
Cysteine						
Other amino acid	5 (26.3%)	0.119*	1 (5.3%)	0.353 <sup>†</sup>	0 (0.0%)	1.000 <sup>‡</sup>
Creating	9 (30.0%)		1 (3.3%)		0 (0.0%)	
Eliminating	30 (47.6%)		7 (11.1%)		2 (3.2%)	
Domain						
cbEGF-like	28 (41.2%)	0.257 <sup>‡</sup>	6 (8.8%)	0.836 <sup>‡</sup>	2 (2.9%)	1.000 <sup>‡</sup>
EGF-like	7 (58.3%)		1 (8.3%)		0 (0.0%)	
Hybrid module	3 (25.0%)		0 (0.0%)		0 (0.0%)	
TGFBP	2 (18.2%)		1 (9.1%)		0 (0.0%)	
4-cys motif LTBP like	4 (50.0%)		1 (12.5%)		0 (0.0%)	
Region						
TGF- $\beta$ regulating	9 (90.0%)	<b>0.033<sup>‡</sup></b>	2 (20.0%)	0.658 <sup>‡</sup>	1 (10.0%)	0.250 <sup>†</sup>
Neonatal region	7 (36.8%)		2 (10.5%)		0 (0.0%)	
TGF- $\beta$ binding	8 (40.0%)		2 (10.0%)		1 (5.0%)	
LTBP	13 (46.4%)		2 (7.1%)		0 (0.0%)	
C-N interaction site	0 (0.0%)		0 (0.0%)		0 (0.0%)	

ATN = atrophic, tractional, and neovascular maculopathy; cbEGF = calcium-binding epidermal growth factor; *FBN1* = fibrillin-1; LTBP = latent transforming growth factor  $\beta$  binding protein; MFS = Marfan syndrome; PTC = premature termination codon; TGFBP = transforming growth factor  $\beta$  binding protein; TGF- $\beta$  = transforming growth factor  $\beta$ .

Bold type indicates *P* values less than 0.05.

\*Pearson chi-squared tests.

<sup>†</sup>Yates's correction for continuity.

<sup>‡</sup>Fisher exact test.

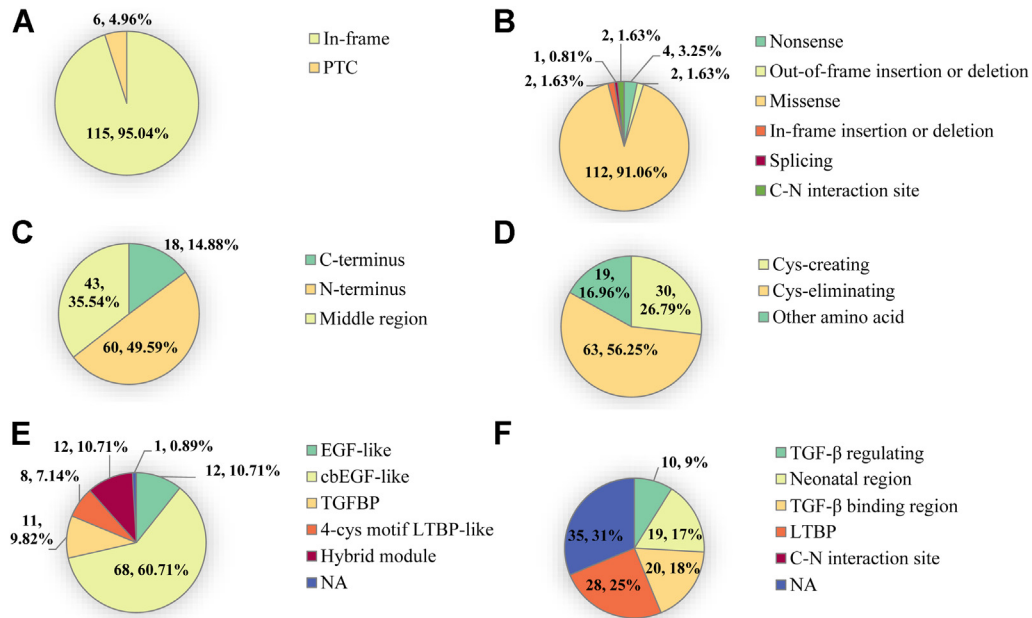


**Figure 4.** Genetic analysis of *FBNI* mutation identified in 121 patients with Marfan syndrome. **A**, Proportions of PTCs and in-frame mutation. **B**, Proportion of missense mutations, insertion or deletion, splicing mutation, intragenic duplication, nonsense mutations, out-of-frame insertion, or deletion mutations and allele deletion mutations. **C**, Proportions of mutations in the N-terminal region (exon 1–21), middle region (exon 22–42), and C-terminal region (exon 43–65). **D**, Proportions of cysteine creating mutation, cysteine eliminating mutations, and NA in missense mutations. **E**, Proportions of mutations in EGF-like domain, cbEGF-like domain, TGFβP domain, 4-Cys motif LTBP-like domain, hybrid module, and NA within missense mutation. **F**, Proportions of mutations in the neonatal region, TGF-β binding region, TGF-β regulating region, LTBP region, C-N interaction site region, and NA within missense mutation. cbEGF = calcium-binding epidermal growth factor; *FBNI* = fibrillin-1; LTBP = latent transforming growth factor β binding protein; NA = not available; PTC = premature termination codon; TGFβP = transforming growth factor β binding protein; TGF-β = transforming growth factor β.

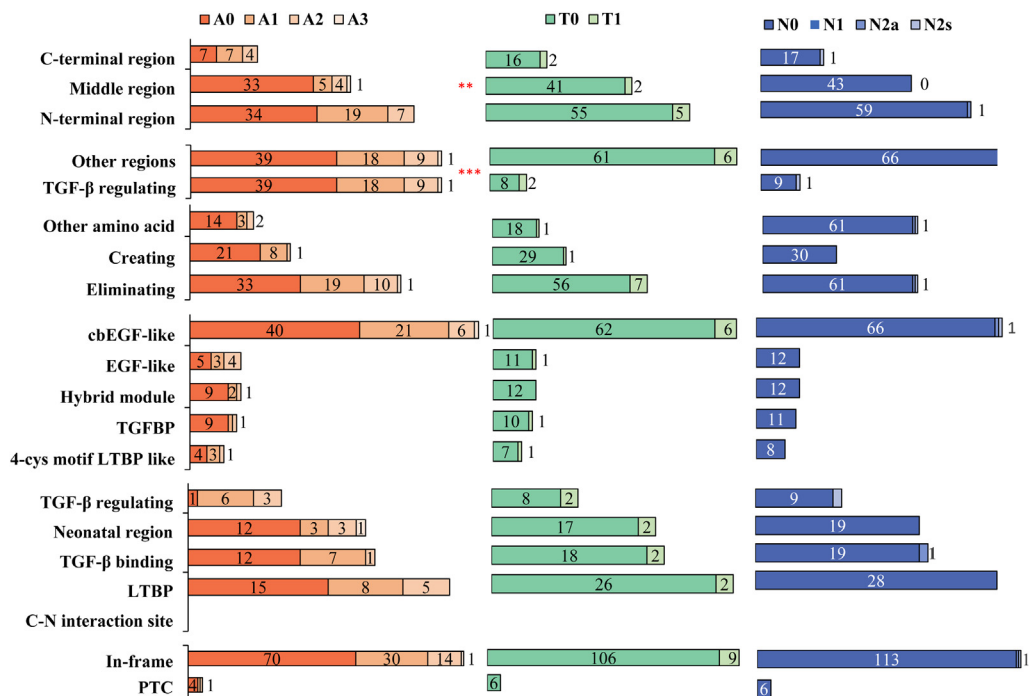


**Figure 5.** The number of patients with mutations in *FBNI* domains with atrophic, tractional, and neovascular maculopathy classification system and the relationship between *FBNI* genotype and maculopathy (atrophic, tractional, and neovascular maculopathy classification system). A = atrophic maculopathy; cbEGF = calcium-binding epidermal growth factor; *FBNI* = fibrillin-1; LTBP = latent transforming growth factor β binding protein; N = neovascular maculopathy; PTC = premature termination codon; T = tractional maculopathy; TGFβP = transforming growth factor β binding protein; TGF-β = transforming growth factor β. \*\*Yates's correction for continuity, \*\*\*Fisher exact test,  $P < 0.05$  are highlighted in red.



observed in some patients with MFS.<sup>44,45</sup> Baldwin et al<sup>46,47</sup> demonstrated that the epithelial-mesenchymal state of retinal pigment epithelial cells influenced their ability to assemble fibrillin microfibrils. Therefore, as demonstrated in our study, there is a correlation between the region of *FBNI* mutations and the incidence of retinopathy. The manifestation of myopic maculopathy resembles the macular features in patients with MFS, prompting the utilization of the ATN classification system to categorize the fundus characteristics in our study cohort.<sup>8,48</sup> Maculopathy was prevalent in over one-third of our patients with MFS, primarily manifesting as atrophy, followed by traction and neovascularization.

Our study revealed a notably higher incidence of PS involvement compared with the general high myopia population (44.63% vs. 13.2%).<sup>8</sup> Only 5 patients with PS did not develop high myopia, and their mutations were exclusively localized to the hybrid module domain and nonfunctional regions. Posterior staphyloma appears linked to aberrations in scleral structure.<sup>49</sup> Major changes in scleral structure including thinning of the sclera at the posterior pole and reduction in collagen fiber diameter in the outer sclera are caused by significant changes in the metabolism of the scleral cellular and extracellular environment. These major metabolic changes involve reduced collagen synthesis, increased collagen degradation, reduced glycosaminoglycan synthesis, altered integrin expression, and decreased fibroblast to myofibroblast differentiation.<sup>49</sup> Due to the extreme thinness of choroid, both the retina and Bruch's membrane closely adhere to the scleral curvature.<sup>48</sup> Furthermore, PS was observed in all patients with tractional

maculopathy. Several researches have reported that the presence of PS plays a key role in traction development.<sup>11,50,51</sup>

This study has several notable strengths. Firstly, it involved a comprehensive analysis of the correlations between posterior segment phenotypes and *FBNI* genotypes. Additionally, the utilization of the ATN system based on the MFS cohort and the inclusion of a diverse patient population with varying degrees of maculopathy enhanced the robustness of our findings. However, it is crucial to discuss the study's limitations. First, the research was conducted at a single center, primarily with patients from eastern China, which may limit the generalizability of our results. Second, the prevalence of macular traction might have been underestimated because of the absence of fluorescein angiography and indocyanine green angiography in our assessments. What's more, the association between mutation and PS or maculopathy remains to be explored. Finally, future investigations should aim to elucidate the mechanisms underpinning these findings, providing a deeper insight into the pathophysiology.

In conclusion, *FBNI* mutations located in the TGF- $\beta$  regulating region and C-terminal region associate with the development of PS and maculopathy, and tend to result in more severe phenotypes. Mutations affecting the TGF- $\beta$  regulating region alter TGF- $\beta$  signaling, increasing collagen fibers and thereby promoting fibrosis. These changes contribute to decreased retinal elasticity, tortuous retinal vessels, scleral structural abnormalities, and elongation of AL. Our findings have important implications for the diagnosis and management of MFS. Further research is required to validate and expand our findings while delving deeper into the molecular mechanisms at play.

## Footnotes and Disclosures

Originally received: December 5, 2023.

Final revision: March 25, 2024.

Accepted: April 1, 2024.

Available online 6 April 2024. Manuscript no. XOPS-D-23-00312.

<sup>1</sup> Eye Institute and Department of Ophthalmology, Eye & ENT Hospital, Fudan University, Shanghai, China.

<sup>2</sup> NHC Key Laboratory of Myopia, Fudan University, Shanghai, China.

<sup>3</sup> Key Laboratory of Myopia, Chinese Academy of Medical Sciences, Shanghai, China.

<sup>4</sup> Shanghai Key Laboratory of Visual Impairment and Restoration, Shanghai, China.

\*Y.L. and Y.J. contributed equally as co-first authors.

Disclosure(s):

All authors have completed and submitted the ICMJE disclosures form.

The author(s) have made the following disclosure(s):

Financial support provided by National Natural Science Foundation of China (Grant no. 82271068) and Shanghai Science and Technology Commission (Grant no. 22Y11910400) (Y.-x.J.).

**HUMAN SUBJECTS:** Human subjects were included in this study. This retrospective clinical observational study adhered to the principles outlined in the Declaration of Helsinki and received approval from the Human Research Ethics Committee of the Eye and ENT Hospital of Fudan University (ChiCTR2000039132). Written informed consent was obtained from all participants or their guardians in subjects <18 years old.

No animal subjects were included in this study.

Author Contributions:

Conception and design: Liu, Ju, Chen, Jiang

Analysis and interpretation: Liu, Ju, Chen, Jiang

Data collection: Liu, Ju

Obtained funding: Jiang

Overall responsibility: Liu

Abbreviations and Acronyms:

**AL** = axial length; **ATN** = atrophic, tractional, and neovascular maculopathy; **cbEGF** = calcium-binding epidermal growth factor; **CI** = confidence interval; **EL** = ectopia lentis; **FBNI** = fibrillin-1; **LTBP** = latent transforming growth factor  $\beta$  binding protein; **MFS** = Marfan syndrome; **OR** = odds ratio; **PS** = posterior staphyloma; **RD** = retinal detachment; **TGF- $\beta$**  = transforming growth factor  $\beta$ .

Keywords:

*FBNI*, Genotype-phenotype correlation, Maculopathy, TGF- $\beta$  regulating sequence.

Correspondence:

Tian-hui Chen, MM, Department of Ophthalmology, Eye and ENT Hospital of Fudan University, 83 Fenyang Rd, Shanghai 200031, China. E-mail: [chentianhui97@163.com](mailto:chentianhui97@163.com); and Yong-xiang Jiang, MD, PhD, Department of Ophthalmology, Eye and ENT Hospital of Fudan University, 83 Fenyang Rd, Shanghai 200031, China. E-mail: [yongxiang\\_jiang@163.com](mailto:yongxiang_jiang@163.com).

## References

- Kjeldsen S, Andersen N, Groth K, et al. Ocular morbidity in Marfan syndrome: a nationwide epidemiological study. *Br J Ophthalmol*. 2023;107:1051–1055.
- Kumar A, Agarwal S. Marfan syndrome: an eyesight of syndrome. *Meta Gene*. 2014;2:96–105.
- Dietz H. FBN1-related Marfan syndrome. In: Adam MP, Mirzaa GM, Pagon RA, et al., eds. *GeneReviews*<sup>®</sup> [Internet]. Seattle, WA: University of Washington, Seattle; 2001:1993–2023.
- Remulla JF, Tolentino FI. Retinal detachment in Marfan's syndrome. *Int Ophthalmol Clin*. 2001;41:235–240.
- Sehgal P, Narang S, Chandra D. Rhegmatogenous retinal detachment with giant retinal tear in a child with Marfan's syndrome: a rare ocular emergency. *BMJ Case Rep*. 2021;14:e241354.
- Stephenson KAJ, Dockery A, O'keefe M, et al. A FBN1 variant manifesting as non-syndromic ectopia lentis with retinal detachment: clinical and genetic characteristics. *Eye (Lond)*. 2020;34:690–694.
- Nie F, Ouyang J, Tang W, et al. Posterior staphyloma is associated with the microvasculature and microstructure of myopic eyes. *Graefes Arch Clin Exp Ophthalmol*. 2021;259:2119–2130.
- Ohno-Matsui K, Lai TY, Lai CC, Cheung CM. Updates of pathologic myopia. *Prog Retin Eye Res*. 2016;52:156–187.
- Gariano RF, Kim CH. Evaluation and management of suspected retinal detachment. *Am Fam Physician*. 2004;69:1691–1698.
- Chen H, Ng KY, Li S, et al. Characteristics OF the foveal microvasculature in children with Marfan syndrome: an optical coherence tomography angiography study. *Retina*. 2022;42:138–151.
- Chen ZX, Jia WN, Jiang YX. Genotype-phenotype correlations of Marfan syndrome and related fibrillinopathies: phenomenon and molecular relevance. *Front Genet*. 2022;13:943083.
- Sheikhzadeh S, Kade C, Keyser B, et al. Analysis of phenotype and genotype information for the diagnosis of Marfan syndrome. *Clin Genet*. 2012;82:240–247.
- Stark VC, Hensen F, Kutsche K, et al. Genotype-phenotype correlation in children: the impact of FBN1 variants on pediatric Marfan care. *Genes (Basel)*. 2020;11:799.
- Chen Z, Chen T, Zhang M, et al. Fibrillin-1 gene mutations in a Chinese cohort with congenital ectopia lentis: spectrum and genotype-phenotype analysis. *Br J Ophthalmol*. 2022;106:1655–1661.
- Chen ZX, Chen TH, Zhang M, et al. Correlation between FBN1 mutations and ocular features with ectopia lentis in the setting of Marfan syndrome and related fibrillinopathies. *Hum Mutat*. 2021;42:1637–1647.
- Franken R, Teixeira-Tura G, Brion M, et al. Relationship between fibrillin-1 genotype and severity of cardiovascular involvement in Marfan syndrome. *Heart*. 2017;103:1795–1799.
- Stengl R, Agg B, Polos M, et al. Potential predictors of severe cardiovascular involvement in Marfan syndrome: the emphasized role of genotype-phenotype correlations in improving risk stratification—a literature review. *Orphanet J Rare Dis*. 2021;16:245.
- Chen J, Jing Q, Tang Y, et al. Corneal curvature, astigmatism, and aberrations in Marfan syndrome with lens subluxation: evaluation by pentacam HR system. *Sci Rep*. 2018;8:4079.
- Chen J, Jing Q, Tang Y, et al. Age differences in axial length, corneal curvature, and corneal astigmatism in Marfan syndrome with ectopia lentis. *J Ophthalmol*. 2018;2018:1436834.
- Chen J, Tang Y, Jing Q, et al. Analysis of corneal spherical aberrations in Chinese bilateral ectopia lentis patients. *Front Med (Lausanne)*. 2021;8:736686.
- Groth KA, Von Kodolitsch Y, Kutsche K, et al. Evaluating the quality of Marfan genotype-phenotype correlations in existing FBN1 databases. *Genet Med*. 2017;19:772–777.
- Perlee LT, Bansal AT, Gehrs K, et al. Inclusion of genotype with fundus phenotype improves accuracy of predicting choroidal neovascularization and geographic atrophy. *Ophthalmology*. 2013;120:1880–1892.
- Loeys BL, Dietz HC, Braverman AC, et al. The revised Ghent nosology for the Marfan syndrome. *J Med Genet*. 2010;47:476–485.
- Chen T, Chen J, Jin G, et al. Clinical ocular diagnostic model of Marfan syndrome in patients with congenital ectopia lentis by pentacam AXL system. *Transl Vis Sci Technol*. 2021;10:3.
- Chen TH, Chen ZX, Zhang M, et al. Combination of panel-based next-generation sequencing and clinical findings in congenital ectopia lentis diagnosed in Chinese patients. *Am J Ophthalmol*. 2022;237:278–289.
- Flitcroft DI, He M, Jonas JB, et al. IMI - defining and classifying myopia: a proposed set of standards for clinical and epidemiologic studies. *Invest Ophthalmol Vis Sci*. 2019;60:M20–M30.
- Chen Q, He J, Hu G, et al. Morphological characteristics and risk factors of myopic maculopathy in an older high myopia population-based on the new classification system (ATN). *Am J Ophthalmol*. 2019;208:356–366.
- Liu Y, Chen T, Jiang Y. What should we pay more attention to Marfan syndrome expecting ectopia lentis: incidence and risk factors of retinal manifestations. *J Pers Med*. 2023;13:398.
- Chaudhry SS, Cain SA, Morgan A, et al. Fibrillin-1 regulates the bioavailability of TGFbeta1. *J Cell Biol*. 2007;176:355–367.
- Chen ZX, Chen JH, Zhang M, et al. Analysis of axial length in young patients with Marfan syndrome and bilateral ectopia lentis by Z-scores. *Ophthalmic Res*. 2021;64:811–819.
- Yuan SM, Jing H. Marfan's syndrome: an overview. *Sao Paulo Med J*. 2010;128:360–366.
- Zeigler SM, Sloan B, Jones JA. Pathophysiology and pathogenesis of Marfan syndrome. *Adv Exp Med Biol*. 2021;1348:185–206.
- Landis BJ, Veldtman GR, Ware SM. Genotype-phenotype correlations in Marfan syndrome. *Heart*. 2017;103:1750–1752.
- Latasiewicz M, Fontecilla C, Milla E, Sanchez A. Marfan syndrome: ocular findings and novel mutations-in pursuit of genotype-phenotype associations. *Can J Ophthalmol*. 2016;51:113–118.
- Garg A, Xing C. De novo heterozygous FBN1 mutations in the extreme C-terminal region cause progeroid fibrillinopathy. *Am J Med Genet A*. 2014;164A:1341–1345.
- Jensen SA, Aspinall G, Handford PA. C-terminal propeptide is required for fibrillin-1 secretion and blocks premature assembly through linkage to domains cbEGF41-43. *Proc Natl Acad Sci U S A*. 2014;111:10155–10160.
- Zhang M, Sun S, Wang L, et al. Zonular defects in lox11-deficient zebrafish. *Clin Exp Ophthalmol*. 2022;50:62–73.

38. Zhang M, Chen Z, Chen T, et al. Cysteine substitution and calcium-binding mutations in FBN1 cbEGF-like domains are associated with severe ocular involvement in patients with congenital ectopia lentis. *Front Cell Dev Biol.* 2021;9: 816397.
39. Ruiz-Moreno JM, Puertas M, Flores-Moreno I, et al. Posterior staphyloma as determining factor for myopic maculopathy. *Am J Ophthalmol.* 2023;252:9–16.
40. Nistala H, Lee-Arteaga S, Smaldone S, et al. Fibrillin-1 and -2 differentially modulate endogenous TGF-beta and BMP bioavailability during bone formation. *J Cell Biol.* 2010;190: 1107–1121.
41. Ghazi NG, Green WR. Pathology and pathogenesis of retinal detachment. *Eye (Lond).* 2002;16:411–421.
42. Hachana S, Larrivee B. TGF-Beta superfamily signaling in the eye: implications for ocular pathologies. *Cells.* 2022;11: 2336.
43. Stone WL, Patel BC, Basit H, Salini B. Retinopathy. In: *StatPearls*. Treasure Island, FL: StatPearls Publishing LLC; 2023;2.
44. Alonso F, Li L, Fremaux I, et al. Fibrillin-1 regulates arteriole integrity in the retina. *Biomolecules.* 2022;12:1336.
45. Di Marino M, Cesareo M, Aloe G, et al. Retinal and choroidal vasculature in patients with Marfan syndrome. *Transl Vis Sci Technol.* 2020;9:5.
46. Eckersley A, Mellody KT, Pilkington S, et al. Structural and compositional diversity of fibrillin microfibrils in human tissues. *J Biol Chem.* 2018;293:5117–5133.
47. Ohman T, Gawriyski L, Miettinen S, et al. Molecular pathogenesis of rhegmatogenous retinal detachment. *Sci Rep.* 2021;11:966.
48. Ruiz-Medrano J, Montero JA, Flores-Moreno I, et al. Myopic maculopathy: current status and proposal for a new classification and grading system (ATN). *Prog Retin Eye Res.* 2019;69:80–115.
49. McBrien NA. Regulation of scleral metabolism in myopia and the role of transforming growth factor-beta. *Exp Eye Res.* 2013;114:128–140.
50. Berger W, Kloeckener-Gruissem B, Neidhardt J. The molecular basis of human retinal and vitreoretinal diseases. *Prog Retin Eye Res.* 2010;29:335–375.
51. Cheong KX, Xu L, Ohno-Matsui K, et al. An evidence-based review of the epidemiology of myopic traction maculopathy. *Surv Ophthalmol.* 2022;67:1603–1630.

## Genotype-phenotype Correlations of Ocular Posterior Segment Abnormalities in Marfan Syndrome

000

Yan Liu, BM, Yuqiao Ju, MM, Tian-hui Chen, MM, Yong-xiang Jiang, MD, PhD

In this study of 121 patients with Marfan syndrome with *FBNI* mutations, maculopathy and posterior staphyloma correlated with mutation location and region. Notably, mutations in the TGF- $\beta$  regulating sequence increased retinopathy risk.